

The potential impacts of plastic on the marine carbon cycle

Received: 20 April 2024

Accepted: 15 August 2025

Published online: 18 September 2025

 Check for updates

Qiaotong Pang¹, Peipei Wu², Luisa Galgani^{3,4}, Xinle Wang¹, Ziman Zhang¹, Tengfei Yuan⁵, Haikun Wang¹ & Yanxu Zhang⁵✉

Increasing plastic waste has triggered global concerns for the potential detrimental effects on marine ecosystems. The impact of plastic reaches beyond the immediate harm to marine life to encompass the marine biogeochemical cycle and the global carbon budget. We investigate these effects by integrating an oceanic plastic simulation with a marine ecosystem model. We find that oceanic plastic could disturb the marine carbon cycle through three pathways: the plastic carbon buried in sediments, the release of dissolved organic carbon from water-column plastic and the toxicity effect on marine phytoplankton. Our scenario analysis suggests that there are 0.70 (0.13–3.8) Tg of plastics entering the ocean every year, however, the overall impact of oceanic plastics on decreasing ocean carbon uptake could reach 12.1 TgC yr⁻¹. Our model predicts that the global plastic released into the ocean could result in up to 1.6 PgC of lost ocean carbon uptake and storage by 2050, given the foreseeable growth of plastic production and its long-lasting impacts. We urge comprehensive control policies to mitigate the losses caused by marine plastics both in ecosystem integrity and addressing climate change.

The rampant consumption of plastics has raised concerns about the sustainable future of the world because of the immense volumes of plastic waste and the diverse damages they inflict on various environments. The ocean, in particular, is severely affected, with millions of metric tons of plastic waste entering through various pathways, including river transport, atmospheric deposition, shipping, fishing activities and beach littering^{1,2}. Plastic wastes disperses horizontally and vertically throughout the ocean, driven by the interplay of buoyancy, gravity, wind and ocean currents^{3,4}. Oceanic plastics pose threats to marine life, including entanglement of sea turtles, the asphyxiation of seabirds and the toxic impacts on fishes⁵. Plastic pollution also affects marine microorganisms and the carbon cycle, further complicating our efforts to achieve sustainable development goals concerning plastics⁶. However, the pattern and magnitude of these impacts as well as their overall effect on the ocean and the world remain yet to be clearly quantified and understood.

The ocean, as the largest carbon reservoir, contains diverse forms of organic and inorganic carbon distributed in sediments, marine organisms and seawater^{7,8}. Under the combined effects of ocean currents and the plastic biomass aggregation, oceanic plastics embedded into marine snow can sink at rates of 1.4–152 m per day (ref. 9). The sinking rate is not only influenced by the density of plastics but also by the density of plastic biomass aggregates^{10,11}. A considerable amount of carbon is buried in the marine system, such as 200 TgC yr⁻¹ in marine sediments, 200–350 TgC yr⁻¹ in coastal sediments, as well as 74.4–124.2 Tg of organic carbon sequestered by the blue carbon system every year^{12–14}. The sinking of biofouled plastics and non-biofouled plastics can contribute an additional 7.8 TgC to the ocean and coasts sediments every year (ref. 15). Meanwhile, the remaining plastics could continuously release dissolved organic carbon (DOC) which can be used by marine microorganisms and directly incorporated into the marine carbon cycle¹⁴.

¹School of Atmospheric Sciences, Nanjing University, Jiangsu, China. ²Scripps Institution of Oceanography, University of California San Diego, La Jolla, CA, USA. ³Environmental Spectroscopy Group, Department of Biotechnology, Chemistry and Pharmacy, University of Siena, Siena, Italy.

⁴National Biodiversity Future Center, Palermo, Italy. ⁵Department of Earth and Environmental Science, Tulane University, New Orleans, LA, USA.

✉e-mail: yzhang127@tulane.edu

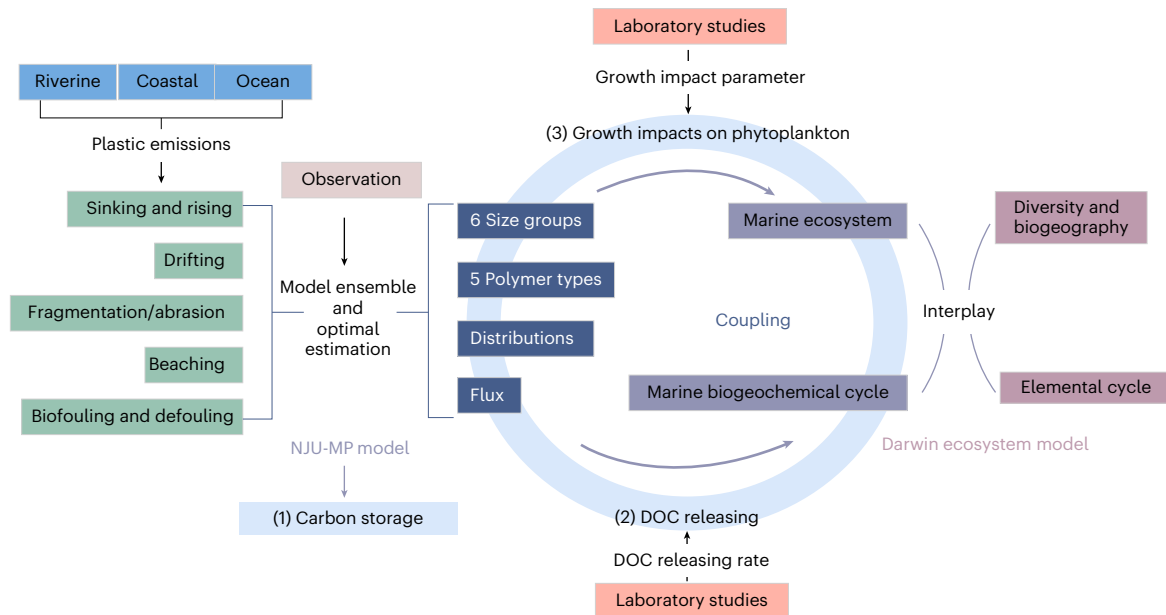


Fig. 1 | Framework of the NJU-MP model and the Darwin ecosystem model coupling. The NJU-MP model simulate the distribution of plastics with different polymer types and sizes in the ocean. The Darwin ecosystem model is used

to examine the potential impacts of plastics on the marine carbon cycle by combining the distribution of oceanic plastics with experimental data from laboratory studies as inputs.

Plastics could alter the grazing behaviour of zooplankton, impacting the phytoplankton biomass and carbon uptake, as suggested by previous studies^{15,16}. Laboratory studies, often conducted at plastic concentrations higher than marine ones, suggest that plastics could also directly impact marine phytoplankton by increasing oxidative stress, altering cell morphology and diminishing chlorophyll levels^{17,18}. These combined effects result in inhibited growth and photosynthesis of phytoplankton because of toxicity effects of plastics on plankton cells^{19,20}. The extent of such impairments varies depending on the plastics composition, phytoplankton species and phytoplankton growth characteristics^{18,20–26}, with the global impact remaining unknown. Given the pivotal role phytoplankton plays in supporting the whole marine ecosystem by supplying oxygen and nutrition, we propose that the cumulative growth impairments experienced by individual phytoplankton have the potential to alter the ocean biogeochemistry and carbon cycles including the uptake of CO₂.

Here we develop a coupled ocean plastic and marine ecosystem model to assess the comprehensive impacts of oceanic plastics on the marine phytoplankton community and the carbon cycle as illustrated in Fig. 1. We use a global ocean plastic simulation based on a three-dimensional model, the Nanjing University marine plastic model (NJU-MP)¹. This model provides a detailed and comprehensive simulation of the behaviours of plastic particles in the ocean, accounting for variations in chemical compositions and sizes, including processes such as sinking, rising, drifting, beaching and biofouling. Furthermore, it evaluates the uncertainties associated with these processes using an ensemble model approach. The model also assimilates available surface ocean plastic observations and considers the uncertainty associated with different plastic discharge inventories. The model performs reasonably well in simulating oceanic plastic concentrations, with an R^2 value of 0.38 and a root mean square error of 0.53 with a unit of $\log(\text{g km}^{-2})$ when comparing modelled and observed surface oceanic plastic mass concentrations¹. We use the simulated plastic distribution in the global ocean, based on emissions accumulated from 1950 to 2020, as input for marine ecosystem modelling. We examine the comprehensive impact of plastics such as DOC-releasing and toxicity effects on marine phytoplankton by using the Darwin ecosystem model, which simulates interactions between marine plankton

community and nutrients (for example, carbon, nitrogen, phosphorus, silica, iron and related compounds)^{7,25}. It incorporates the growth, grazing and mortality of different plankton functional groups (including diatoms, other large plankton, *Prochlorococcus*, *Synechococcus*, coccolithophores and diazotrophs) and reproduces observed global ocean plankton community structure. We include plastic-released DOC as a new DOC source and adjust phytoplankton growth rates on the basis of the toxicity relationship between plastics and phytoplankton in the model. Subsequently, these impacts are translated into changes in CO₂ flux from the sea to the air, and we account for the contribution of oceanic plastic waste into the global carbon budget. Given that our simulations are jointly driven by several results and parameters related to interactions between oceanic plastics, marine ecosystems and marine biogeochemical cycles, we have designed various scenarios to address the range of uncertainties. We evaluate the negative impacts of oceanic plastics on the basis of results from all scenarios and discuss potential strategies to mitigate these impacts.

Plastic carbon buried in sediments and beaches

Our model suggests that buried oceanic plastics could be stored in ocean sediments and beaches, which are relatively stable but non-reactive in the marine biogeochemical cycle and do not remove from the contemporary atmospheric carbon pool⁶. By modelling the spatial distribution of oceanic plastic in both sediments and beaches, we find that approximately 0.13 Tg and 0.21 Tg of carbon are buried in sediments and beaches in 2020 in our plastic abundance scenario (middle) (Methods gives more details about scenarios setting), respectively (Fig. 2a,b). The sedimentary process of oceanic plastics in our model is driven by the sinking process and affected by the biofouling process that alters the densities of plastics (Methods). Although the sinking and storage of plastics in sediments are not part of the ocean plankton biological pump, plastics and particulate organic matters such as marine snow can combine together and mutually affect their sink processes^{6,10}. Sediments shallower than 100 m receive more than 75% of the total sedimented plastic fluxes (Fig. 2d). The simulated buried carbon from sedimented plastics is higher in the nearshore water areas with shallow depth and high plastic emission from land, such as the east and south-east coasts, the high-latitude Atlantic and the Arctic (Fig. 2a). Similarly,

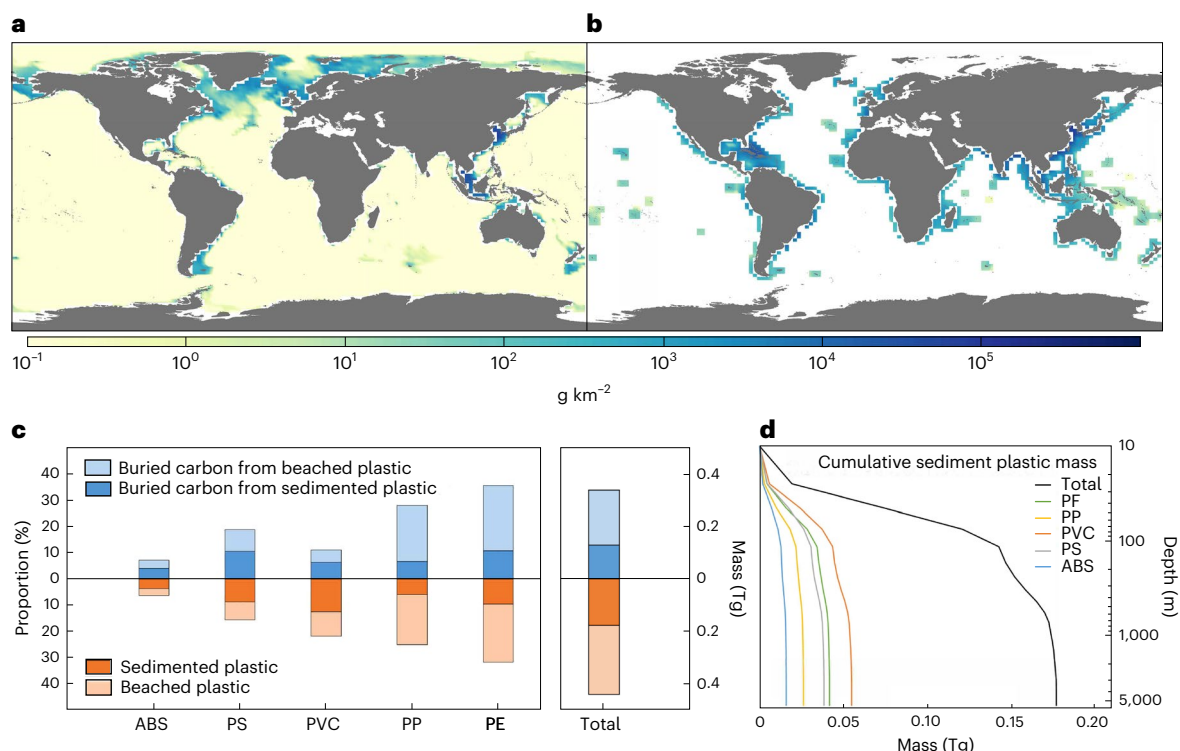


Fig. 2 | Plastic carbon buried in sediments and beaches. **a,b**, Modelled spatial distribution of buried carbon from sedimented plastics (0.13 TgC yr^{-1}) (**a**) and beached plastics (0.21 TgC yr^{-1}) (**b**) (The color bar from light yellow to deep blue indicates the range of concentration changes of buried carbon, from 10^{-1} to 10^5 g km^{-2}). **c**, Proportion and mass of different polymer types of plastics and

their contributions to buried carbon. **d**, Vertical cumulative mass of sedimented plastic with different depths under the sea surface (we chose carbon storage in 2020 as the baseline of current annual buried carbon from oceanic plastics). Basemaps in **a** and **b** from Natural Earth (<https://www.naturalearthdata.com>).

beached plastics are predominantly found in nearshore regions with higher plastic emissions, such as the populated mid-latitude regions (Fig. 2b). Favourable beach morphology, especially gentle nearshore slopes and sandy coasts facilitates the beaching of oceanic plastics, leading to notable increase of buried carbon in the Caribbean sea as well as in the Southeast Asian seas²⁷.

We find that the buried carbon from oceanic plastics is affected by polymer types, with each polymer type differing in density and carbon content. Our simulation includes five polymer types: polyethylene (PE), polypropylene (PP), polyvinyl chloride (PVC), polystyrene (PS) and acrylonitrile butadiene styrene (ABS) plastic. These polymers represent more than 61% of global plastic production up to 2015, with the exception of ABS²⁸. The contribution of different polymers to buried carbon closely mirrors their emission levels (Fig. 2c). Specifically, PE and PP are the leading polymer in global plastic production, usage and wastes²⁸, which contribute 32% and 25% to total sedimented and beached plastics and 35% and 28% of buried plastic carbon, respectively. Plastics with a relatively high density such as PVC (1.38 g cm^{-3}) and PS (1.05 g cm^{-3}) exhibit faster sinking velocities, leading to their higher contributions to the total sedimented and beached plastics (22% and 15%, respectively) compared to their emissions (5% and 6%, respectively)²⁸. However, the contribution of PVC to the buried carbon is sharply reduced (11%), attributable to its lower carbon content compared to other polymer types.

Released DOC from seawater plastic

Our simulation reveals that oceanic plastics could disrupt the marine carbon cycle by releasing 0.25 TgC yr^{-1} of DOC into the global ocean (on the basis of modelling results of 2020), which is around 63% of Romera-Castillo et al.'s estimation¹⁶. We incorporate a plastic DOC release process mediated by solar radiation in the ocean ecosystem

model (Methods). In general, the distribution of plastic-released DOC mirrors the spatial patterns of seawater plastics (Fig. 3a), with higher concentrations over the centre of mid-latitude gyres, also called garbage patches, including the North Pacific, South Pacific, North Atlantic, South Atlantic and Indian Ocean²⁹. The coastal regions of Asia, Europe and North and South America also experience higher DOC releases as a result of riverine and coastal plastic emissions^{30–32}. The plastic-released DOC, largely treated the same as the plankton-derived DOC, affects the carbon biogeochemical cycle by both providing an extra carbon source for microbial respiration and increasing the existed organic carbon content of seawater, which may further influence the sea-to-air CO_2 exchange¹⁹ (Methods). We calculate the increase in oceanic CO_2 flux from the sea to the air caused by plastic-released DOC (Fig. 3b). Our model reveals that plastic-released DOC weakens global oceanic CO_2 uptake by $0.0044 \text{ TgC yr}^{-1}$ (Fig. 3b). The increase in CO_2 flux due to released DOC largely overlaps with the spatial distribution of the DOC but is more concentrated in the mid- and low-latitude oceans. This reflects differences in seawater chemical factors such as pH value and the buffer capacity, as well as the metabolic activity of marine organisms primarily mediated by the temperature⁷. While the increased organic carbon from oceanic plastics could potentially contribute to ocean acidification as an added carbon source, the impact on ocean acidification is currently negligible at present plastic concentrations. Our modelling results suggest that the change of the concentration of hydrogen ions (H^+) due to plastic-released DOC is less than 0.001% even in oceanic areas with high plastic abundance such as the North Pacific garbage patch.

Toxicity effects on phytoplankton communities

Ocean plastics could harm marine phytoplankton because of their toxicity effects, with further implications on the marine carbon cycle

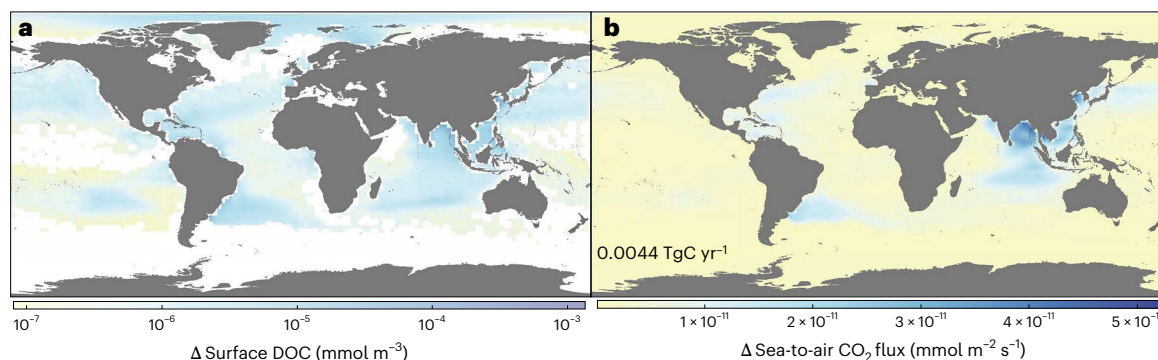


Fig. 3 | Impacts of DOC released by marine plastic on the ocean carbon cycle. a, Sea surface DOC change. **b,** Sea-to-air CO₂ flux change. Basemaps in **a** and **b** from Natural Earth (<https://www.naturalearthdata.com>).

(Fig. 4). We combine the marine ecosystem model with the oceanic plastic simulation by considering the plastic toxicity effect on the growth of phytoplankton (Methods). In the ecosystem model, diatoms, other large plankton (large fast-growing eukaryotes other than diatoms)⁷, *Synechococcus* and *Prochlorococcus* with varying sizes, affinity to different nutrients and growth rate, are selected as representative function groups of the marine phytoplankton communities because of their crucial roles in marine net primary production and oceanic CO₂ uptake^{7,33}. The distributions of the biomass of these four marine phytoplankton groups without the influence of plastics are illustrated in Fig. 4a(i)–(iv). Diatoms, with high affinity to silica, predominantly inhabit high-nutrient waters such as the middle and high-latitude regions of the Atlantic, Indian Ocean and Pacific Ocean. In contrast, other large plankton are relatively more concentrated in the Arctic Ocean according to our simulation. *Synechococcus*, which shares similar habitat preferences with diatoms, is more abundant along the northern coast of the Indian Ocean³⁴. *Prochlorococcus*, with the smallest size, has a complementary distribution to diatoms and *Synechococcus*. It is abundant in the open ocean between 40° N and 40° S as a result of it being outcompeted by other phytoplankton in high-nutrient waters³⁴. The vertical distribution of both oceanic plastics and marine phytoplankton are considered in our model as both of them are three-dimensionally distributed in our model. We only discuss the overall growth change of phytoplankton within the top 100 m because of the concurrent presence of phytoplankton and plastics.

We find distinct spatial patterns for the toxicity effects of oceanic plastics, contingent on the plastic abundance and plankton community structures. We first assess changes in phytoplankton growth resulting from plastic toxicity and competition within the marine phytoplankton community in the combined toxicity effect scenario (maximum) scenario (Fig. 4b(i)–(iv)), which considers the combined toxicity effects of all plastic types. This scenario is categorized into maximum, middle and minimum scenarios by selecting maximum, middle and minimum toxicity effect parameters, respectively, given their substantial variability in literature (Methods). The results suggest that the phytoplankton growth is more severely impacted in plastic-abundant areas including the Pacific garbage patches, the western subtropical Pacific Ocean (particularly the coastal regions), the subtropical Atlantic Ocean and the North Indian Ocean. Although all phytoplankton are affected in those plastic-abundant areas, those impacts are further intensified, mitigated or even reversed, as a result of community competition, as reflected in the growth change rate of the four phytoplankton functional groups (Fig. 4b(i)–(iv)). For example, diatoms and *Synechococcus* dominant in the Pacific garbage patch, exhibit contrasting responses due to community competition and toxicity effects from different plastics. The Pacific garbage patch can be divided into two areas (hereafter referred to as the west and

east, Fig. 4b(i)–(iv)) on the basis of the opposite distribution of plastic concentration and phytoplankton biomass. Phytoplankton is more abundant in the west, while the concentration of plastics is considerably higher in the east due to PE and PP (Supplementary Figs. 8 and 11). The growth of *Synechococcus* in the west is inhibited by relatively high concentrations of PVC, PS and ABS. This leads to increased NO₃ and PO₄ concentrations due to decreased absorption by *Synechococcus*. The favourable nutrient condition largely mitigates the negative effects of plastics on diatoms, resulting in increased growth rate and biomass (–12% as shown in Fig. 4b(i)). These growth changes also contribute to an increase in total biomass of the phytoplankton community. On the contrary, a much higher concentration of plastics in the east restricts the growth of both diatoms and *Synechococcus*, particularly the former with a maximum decrease of –4%. The concentrations of NO₃ (0.44%) and PO₄ (0.10%) are slightly elevated in the west, promoting the growth of *Prochlorococcus*, but there remains a net decrease in the total biomass of the phytoplankton community.

Similar growth change patterns of phytoplankton impacted by oceanic plastics can also be found in other areas such as the east and southeast Asian coastal areas, the subtropical ocean areas and the north Indian ocean areas. The east Asian coastal area, characterized by high plastic abundance, is also the main habitat of diatoms, *Synechococcus* and *Prochlorococcus*. However, our modelling results suggest distinct changes in the growth pattern of these groups. Diatoms suffers from the impairments of several polymer types of oceanic plastics as their growth decreases by more than 1%. Conversely, the growth of *Synechococcus* and *Prochlorococcus* benefits from the loss of diatoms there, offsetting the direct toxicity effect by plastics. Moreover, the model also suggests the adverse growth change patterns of other large plankton and *Synechococcus* in the southeast Asian coastal area, another oceanic plastic-abundant sea area. This underscores the regulatory role of community competition in modulating the impact of plastics on different phytoplankton functional groups (Fig. 4b(i)–(iv)). The growth changes of phytoplankton in the Indian Ocean also highlight the role of intergroup competition, with the growth of *Synechococcus* decreasing, while the growth of *Prochlorococcus* increases. Indeed, all phytoplankton types are potential victims of this oceanic plastic intrusion, but the ‘winner’ and ‘loser’ vary across different areas depending on specific biogeochemical characteristics while oceanic plastics are reshaping the phytoplankton community structure and the marine ecosystem.

The toxicity of plastic on phytoplankton may further impact the oceanic CO₂ flux as a result of the growth rate changes. We find a net increase in air-to-sea CO₂ flux of up to 0.82 TgC yr^{–1}, attributed to the toxicity effect of plastics on marine phytoplankton (the combined toxicity effect scenario (maximum scenario, Fig. 4b(v))). Increased CO₂ flux from the ocean to the atmosphere is simulated in the Indian

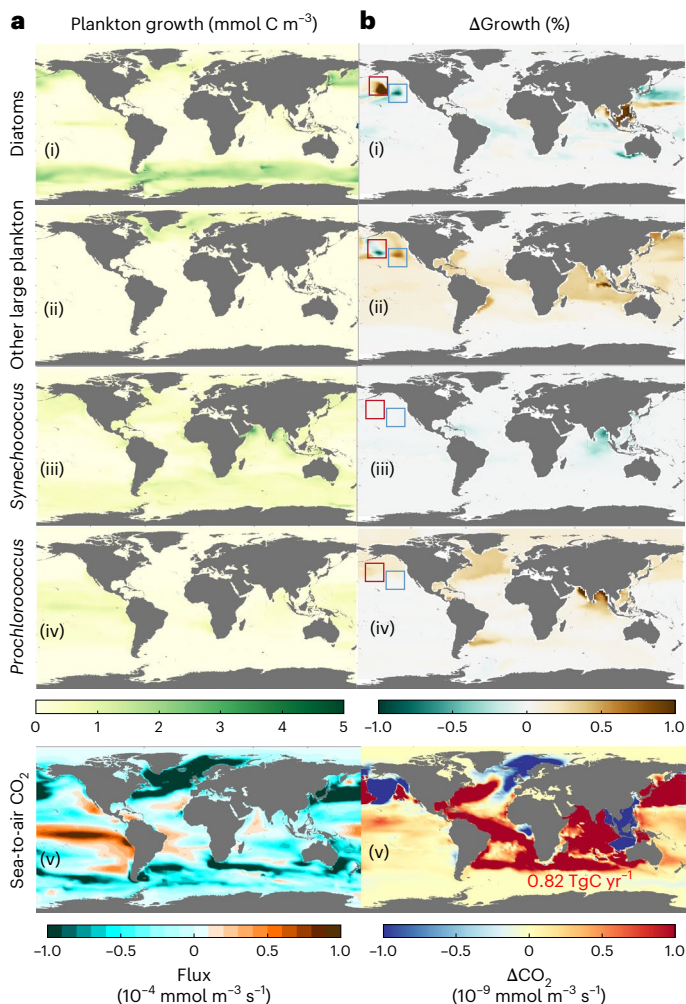


Fig. 4 | Toxicity effect of oceanic plastic on phytoplankton biomass/growth over the top 100 m depth and sea-to-air CO₂ flux. a, Spatial distribution of marine plankton biomass without plastics (i)–(iv). **b**, Phytoplankton growth change in the combined toxicity effect scenario (maximum) (red and blue boxes denote the west and east of the Pacific garbage patch, respectively) (i)–(iv). **a(v)**, Spatial distribution of the mean annual sea-to-air CO₂ flux. **b(v)**, Sea-to-air CO₂ flux change in the combined toxicity effect scenario (maximum). Basemaps in **a** and **b** from Natural Earth (<https://www.naturalearthdata.com>).

Ocean, the Atlantic Ocean and the Northwest Pacific Ocean, while the CO₂ intake flux (that is, from the atmosphere to the ocean) is enhanced in the northeast Pacific Ocean, southeast Asia and the junction of the Atlantic and Arctic Oceans compared to the flux without plastic effects (Fig. 4a(v)). The spatial distribution of oceanic CO₂ uptake changes generally aligns with the overall growth rate changes of different phytoplankton functional groups. Specifically, the varying impairments of oceanic plastics on phytoplankton result in differing impacts on photosynthesis, as indicated by changes in chlorophyll content across different regions. For example, the substantial increase in diatom-related (−7.2%) and *Prochlorococcus*-related (−0.3%) chlorophyll contents due to growth change in the west and east Pacific garbage patch leads to distinct oceanic CO₂ uptake change as shown in Fig. 4b(v). The modelled increase of CO₂ uptake in the southeast Asian coastal area can also be explained by the enhanced photosynthesis of increased other large plankton (−1% increase of other large-related chlorophyll). Similarly, the subtropical ocean areas exhibit prominent CO₂ flux changes as a result of the interplay of toxicity effects from abundant oceanic plastics and the high metabolic activity of phytoplankton in these areas.

Implications

Our simulations are subject to considerable uncertainties. We establish several scenarios to bracket the range of these uncertainties and assess sensitivities of assumptions we make in our simulations, including the abundance of plastics in the ocean, the releasing rate and bioavailability of plastic-released DOC and the dose–effect relationship for the toxicity effects of plastics (Methods and Supplementary Information Text). Using different ocean plastic abundances can notably affect the impacts of plastics on the marine carbon cycle through all three pathways mentioned above (for example, −0.10–3.76 TgC yr^{−1} of oceanic CO₂ uptake change from toxicity effects). Varying the parameters for plastic DOC releasing alters its impacts by a factor of ~4%, whereas different parameters for plastic toxicity have even greater effects on both phytoplankton community and oceanic CO₂ uptake (0.02–0.82 TgC yr^{−1}). Additionally, relative size effect can effectively mitigate the toxicity effects of plastic and their cascading effects (reducing the original impact by 96%). We also examine the interactive effects of these uncertainties, which could lead to a maximum reduction in oceanic CO₂ uptake by 12.08 TgC yr^{−1} (Supplementary Information Text). Despite these uncertainties, our model can still be interpreted as a diagnostic tool and hypothesis generator similar to the ModEx approach (<https://ess.science.energy.gov/modex/>). It helps to reveal potential ways and modes of the interaction between oceanic plastic and the marine carbon cycle. Furthermore, the model results can also guide further experimental and field studies to fill the knowledge gap and reduce model uncertainties.

Plastic is made of crude oil or natural gas and recycled plastic products or plastics sequestered in landfills which are stable enough to hardly release CO₂ to the atmosphere in a decadal timescale. Thus, once buried, most plastic carbon can be assumed to be stable³⁵. However, we find impacts of plastics on the marine ecosystem and carbon cycle. In our simulation, oceanic plastics may reduce oceanic carbon uptake by 0.22 TgC yr^{−1} even in the combined toxicity effect (middle) scenario, which is 31% of oceanic plastic emission (0.70 (0.13–3.8) TgC yr^{−1}) and such impact also ranges from −0.10 to 12.08 TgC yr^{−1} for different scenarios (Supplementary Table 1). It is noteworthy that oceanic plastic pollution and these impacts are long-lasting as a result of the slow degradation rate of plastic in the oceanic environment. The cumulative extra sea-to-air CO₂ flux may reach 0.4 PgC by 2050 (range −0.003–0.4 PgC), a timescale relevant to current climate policies, and most of the released plastic can last even longer, if we assume the ocean plastic emissions remain steady at the present-day level. This value may be further expanded to approximately 1.6 PgC (at maximum), which is between the annual greenhouse gas emissions of the largest (3.0 PgC) and second-largest (1.2 PgC) emitting countries in 2020, as plastic production is increasing at a rate of 8.4% per year (refs. 28,36). There are additional carbon emissions during processes such as plastic production, transport and use, which also have considerable carbon footprint but are not included in this study³⁷. Numerous laboratory studies have demonstrated the notable impacts of plastics on the marine carbon cycle such as 45% reduction in carbon export under relatively high plastic concentrations^{10,38}. With the increase of plastic emission, the impacts of oceanic plastics are even more important in the future, contrasting with likely decreasing or even fully neutralized CO₂ emissions from energy production and other industrial sectors³⁵. Moreover, our results suggest that oceanic plastic debris may have complex impacts on the plankton community structure and primary production, which fuel the ocean ecosystem and have many cascading effects on oceanic CO₂ uptake, O₂ production, fisheries and aquaculture, marine food webs and on vital ecological functions and ecosystem service of the ocean³⁴. Oceanic plastic can also affect various trophic levels in marine ecosystems, including zooplankton³⁹. These effects would further compound and amplify the impact of plastics on the marine carbon cycle and our simulation is relatively conservative.

Oceanic plastic concentrations are generally higher in nearshore areas as it is close to emission sources such as estuaries and coastal cities. Phytoplankton and primary production are also abundant in these areas as a result of nutrient repletion and reduced predation, and CO₂ intakes are correspondingly high in these areas, constituting a substantial blue carbon sink. Nearshore areas are thus potentially a hotspot for the impact of plastics on the ocean ecosystem and carbon cycle. While the resolution of our model is relatively coarse to directly model this impact, similar impact modes and influencing factors as in the open ocean may still apply. Indeed, our current estimation of the impact of oceanic plastic is conservative and we call for further research on this topic.

The varied chemical and physical properties of oceanic plastic polymers lead to difference in their cycle processes and spatial distributions in the ocean, which is also the basis for their varying impacts on the marine carbon cycle. Combined with their distinct toxicological and DOC-releasing characteristics^{14,18,20–26,40,41}, the differing stocks of these oceanic plastics contribute more unevenly to the impact on marine biogeochemistry and carbon cycling. The varied impacts of oceanic plastics are particularly reflected in the heterogeneity of their toxicity effects on different species of phytoplankton. Using PVC and PP as examples, PVC, with its higher density, tends to accumulate more on sediment and beaches than does PP. However, the lower carbon content of PVC reduces its contribution to the buried carbon (less than 40% of the contribution of PP). Meanwhile, although the lower DOC-releasing capacity of PVC (k_{DOC} of PVC is about two orders of magnitude lower than PP) limits its impact on the marine carbon cycle through the DOC pathway, the important ecological toxicity of PVC has resulted in a more noticeable impact on phytoplankton growth and sea-to-air CO₂ exchange compared to PP (Supplementary Fig. 2). Other factors, such as the toxicity effect model and parameters, the relative size effect, the plastic abundance effect and the community competition could further exacerbate the complexity of the potential impacts of plastics on the marine carbon cycle. Higher or lower toxicity effect parameters or plastic abundance could substantially and nonlinearly strengthen or weaken plastics impacts on phytoplankton growth and ocean carbon uptake (Supplementary Figs. 1–4). The particle size can also effectively alter the toxic effect of oceanic plastics on marine phytoplankton, with smaller size plastics generally exerting a greater toxicity effect^{21,42} (Supplementary Fig. 3). Community competition may mitigate the damage of plastics to the growth of specific species of phytoplankton, or exacerbate the growth loss of other phytoplankton, depending on the community structure of the phytoplankton and oceanic plastic concentration at different areas. Although the diversity properties of oceanic plastics and factors mentioned above complicate oceanic plastics effects on the ocean ecosystem and carbon cycle, these also encourage us to implement specific strategies for controlling marine plastic pollution to minimize oceanic plastics impact. Reducing oceanic plastic emissions could effectively reduce the impact on marine ecosystem and ocean carbon uptake. Existing oceanic plastics should be controlled as early as possible before they are washed and worn into smaller microplastics, or even nanoplastics, to prevent their damage to the marine microbial community as well as the marine carbon cycle. Plastic types with higher phytoplankton toxicity and ocean carbon footprint (such as PVC and PS) should be controlled with higher priority. The cleaning up of oceanic plastics in phytoplankton colonies that have notable implications for ocean carbon uptake should be given top priority. Overall, we emphasize the need to consider the impact of plastic debris on ocean biogeochemical and carbon cycle when formulating plastic and climate change policies, such as the ongoing and future negotiation for the global plastic treaty (Intergovernmental Negotiating Committee on Plastic Pollution)⁴³. We suggest that delaying action on plastic pollution might undermine our endeavours to combat climate change, impede our progress towards sustainable development and compromise the functioning of ecosystems and their associated

services. Immediate actions are necessary to mitigate plastic pollution and alleviate its impacts on the carbon cycle and climate change.

Methods

Oceanic plastic simulation

We simulate the transport and transformation of oceanic plastic with different chemical compositions and sizes in the NJU-MP. This model is based on the model framework of MITgcm (Massachusetts Institute of Technology General Circulation Model)⁴⁴. The resolution of NJU-MP is 2° × 2.5° horizontally as well as 22 levels vertically and its time step is 4 h. Five polymer type of oceanic plastics with different densities are included in this model: PE, PP, PVC, PS and ABS, and each of them has six diameter groups: <0.0781, 0.0781–0.3125, 0.3125–1.25, 1.25–5, 5–50 and >50 mm. The model depicts the processes by which plastic waste enters and circulates within the ocean, including sinking and rising, drifting, fragmentation/abrasion, beaching and biofouling and defouling. These processes depend on intrinsic properties of plastic such as density, as well as exterior influences of circulation, marine plankton and so on. The model is run from 1950 to 2020 and the simulated distribution and fluxes of plastic by the end of 2020 are used to further model the impacts of plastics on marine ecosystem as well as marine carbon cycle.

Three plastic emission sources: the riverine plastic emission, the coastal plastic emission and the ocean plastic emission, are used in our oceanic plastic simulation. The riverine plastic emissions are plastic debris carried by river water, so their spatial pattern follows the locations of estuaries from major rivers worldwide³¹. The coastal plastic emissions are closely related to coastal areas, primarily from coastal residents³². Both riverine and coastal emissions derive from terrestrial environment, influenced by factors such as plastic consumption, waste management and population density. Direct ocean plastic emissions refer to plastics discharged from fisheries and shipping and its spatial pattern is consistent with the global footprint of fisheries and shipping tracks^{43,45}. In this simulation, cumulative plastic production is used as a proxy for the historical trend of plastic emissions, with polymer types allocated on the basis of global consumption data in 2013²⁸. Discharged plastics are initially divided into microplastics (<5 mm) and macroplastics (>5 mm) in emission sources, then the diameters groups are expanded to six after fragmentation and abrasion processes of our model.

The sinking and rising of oceanic plastics in our model are determined by their densities, diameters, shapes and the state of seawater. The drifting process, also known as leeway drift or windage, is affected by five forces including gravity, buoyancy, seawater stress, horizontal wind stress and Coriolis force. The fragmentation/abrasion rate varies with the polymer type and shape of oceanic plastics and depends on environmental factors such as sunlight. In our simulation, beaches bidirectionally exchange plastics with the ocean. On the basis of the length of sandy beaches within a model grid, we set an effective beaching rate of 0.15–1.10% per day, with part of beached plastics accumulating over time. In our model, biofouling and defouling are represented as the attachment and release of oceanic plastics with biomass including microbes, phytoplankton, zooplankton and marine snow on the basis of ref. 3. Those processes can change densities of oceanic plastics and further affect the vertical and horizontal transport of oceanic plastics in the sinking, rising and drifting process in our modelling. More details for each process can be found in ref. 1.

Model ensemble and optimal estimation

There are several sources of uncertainty for the plastic emissions simulated by the NJU-MP model. The model parameters and process settings, as well as the oceanic plastic emission sources setting are the main sources of uncertainty. The former includes the value of different parameters in different processes such as the different fragmentation rate (3–30% per year) and varied biofouling rate (based on the biomass data of plankton) for different plastic polymer types¹. The latter

originates from different emission inventories^{34,36,46}. To assess these uncertainties, a model ensemble is constructed by randomly generating model parameters¹. This ensemble consists of 156 modelling scenarios driven by varying model parameters (generated by using a Monte Carlo approach) such as fragmentation, biofouling, sedimentation and beaching rates, as well as emission inventories. These model members are further optimized by constraining them with observation data of ocean surface plastic through a super ensemble three-dimensional variational method¹. The optimized model performs well in capturing the trend of the vertical profile of oceanic plastics¹. The optimal estimates of plastic discharged to the global ocean from these model scenarios range from 0.13 to 3.8 million Mt (metric tons) yr⁻¹, spanning approximately 1.5 orders of magnitudes. We select three scenarios representing minimum (0.13 million Mt yr⁻¹), middle (0.70 million Mt yr⁻¹) and maximum (3.8 million Mt yr⁻¹) estimates of oceanic plastic emission as the minimum, middle and maximum plastic abundances for further modelling of plastic impacts on marine carbon cycle¹.

Marine ecosystem model

We use the Darwin ecosystem model to simulate the impact of plastics on the marine carbon cycle by coupling with the plastic model^{7,33}. The coupled model has the same spatial resolution and time step as the NJU-MP model. The Darwin ecosystem model has been widely used in examining the interplay between marine ecosystem and biogeochemical cycles^{7,47}. Six phytoplankton functional groups (diatom, other large plankton, *Prochlorococcus*, *Synechococcus*, coccolithophores and diazotrophs) and two zooplankton (small and large) functional groups are included to represent the marine plankton community. The biogeochemical cycles of inorganic and organic forms of carbon, nitrogen, phosphate, phosphorus, iron and silica are simulated through the interaction with marine ecosystems. This model also includes the feed, graze and mortality process of marine plankton, as well as the transformation of elements such as the air-to-sea CO₂ exchange process. We select diatoms, other large plankton, *Synechococcus* and *Prochlorococcus* to study the impacts of plastics on the marine ecosystem and carbon cycle. This simulation spans from 2000 to 2020 and we use the results of 2020 as the baseline for further analysis. The Darwin ecosystem model is used to simulate the specific impacts of oceanic plastics on the ocean carbon cycle, including the process and magnitudes, and the structure of coupled model is shown schematically in Fig. 1.

The diversity and biogeography of plankton communities are key for modelling plankton communities. The Darwin ecosystem model explores numerous characteristics such as cell size and nutrient affinity, as well as function traits such as ingestion and growth of phytoplankton to understand them. The Darwin ecosystem model can simulate more complex functions and relationships such as the community competition and top-down control on the basis of basic characteristics and function traits. We simulate the impacts of oceanic plastics on marine phytoplankton communities to understand how plastics impact marine ecosystem. Specifically, we select diatoms, other large plankton, *Synechococcus* and *Prochlorococcus* to investigate the toxicity effect of plastics on the growth of marine phytoplankton community as these four are the major contributors to the total ocean primary productivity and phytoplankton biomass^{34,47}.

The elemental cycle in the Darwin ecosystem model are jointly determined by both biogeochemical transformation and biological activities. For example, inorganic nutrients in surface ocean can finally be transformed as sinking particulates in the sea bed through ingestion, mortality, grazing, egestion of plankton and formation, transformation and remineralization process. We focus on the response of marine carbon cycle to the marine ecosystem change under the impacts of oceanic plastics. Meanwhile, we also treat DOC releasing of plastics as another way of plastics impacting marine carbon cycle by adding plastic-released DOC into oceanic DOC cycle as an extra DOC sources in

the coupled model. These impacts on marine carbon cycle are further examined by the change of oceanic CO₂ uptake.

Buried carbon

Oceanic plastics buried in the ocean sediments are hardly involved in marine biochemical reactions⁶, so we treat them as the increase of buried carbon. Such buried carbon comes from both direct sinking and indirect sinking of plastics resulting from biofouling which can alter the density of plastic. Beached plastics serve as a transfer reservoir of oceanic plastics with part of beached plastics remains and accumulates there. Thus, we also treat beached plastics as a net increase of buried carbon. On the basis of the simulation results of sedimented plastics and beached plastics, we calculate buried carbon from these two sources by multiplying the carbon content of each polymer type of oceanic plastics:

$$C_{\text{sediment}} = \sum \sum P_{ij} A_j C_i \quad (1)$$

where C_{sediment} denotes the mass of buried carbon from sedimented and beached plastics every year (TgC yr⁻¹). Parameter P_{ij} is the concentration of polymer type i of oceanic plastic in grid j (m⁻²) and A_j is the area of grid j . Parameter C_i denotes the percentage of carbon content for five polymer types of oceanic plastics we calculate on the basis of their chemical structures.

DOC releasing

Under light irradiation, oceanic plastics can leach DOC at a certain rate depending on the polymer type of plastics. Plastic-related DOC leaching conforms to zero-order or first-order reaction kinetics^{14,40,41}. To simplify this process, we choose a fixed leaching rate for different polymer types as depicted in Supplementary Table 5. Such release rate drops to a minimum value in the dark environment^{14,40,41}. We treat the rate constant of reaction of plastic DOC leaching as the DOC-releasing rate and calculate the released DOC on the basis of the seawater plastic concentrations and their DOC-releasing rate:

$$P_{\text{DOC}} = P_{ij} k_{\text{DOC}i} \exp(-\text{atten}_j) \text{Bio}_i \quad (2)$$

where P_{DOC} is the concentration of DOC leached from polymer type i of oceanic plastics in grid j with same units as DOC (mmol m⁻³). Parameter $k_{\text{DOC}i}$ denotes the DOC-releasing rate constant of different oceanic plastics and this equation is also modified by atten_j , which is the light irradiation attenuation of each grid attenuated by depth, chlorophyll, planktons and dissolved and particulate material⁴⁸. We first convert DOC-releasing rate from laboratory studies to a rate of uniform light intensity on the basis of their experimental conditions and use the average value of these rates as DOC-releasing rate for each polymer types of plastics under fully illuminated conditions. Then we use the same light attenuation coefficient (atten_j) to represent the percentage of DOC-releasing rate decrease with ocean depth. As few studies measure the DOC-releasing rate of ABS, we use the average value of the DOC-releasing rate of PVC and PS, both amorphous plastics, to represent the DOC-releasing rate of ABS on the basis of their similar chemical and physical properties. We adapt high, middle and low datasets of $k_{\text{DOC}i}$ on the basis of laboratory studies as shown in Supplementary Table 5. Our modelled mean value of total plastic-released DOC is only 0.25 TgC yr⁻¹, which is only nearly 0.0012% of biogenic DOC production rate and 0.0005% of total DOC pool in our model⁴⁹. Thus, we assume plastic-released DOC has the same conversion process as the plankton-derived DOC in our model. Plastic-released DOC in our model can increase the plankton-derived DOC pool and can be used by microbes, ultimately being converted to dissolved inorganic carbon and CO₂ through biological processes within the ocean carbon cycle. On the basis of the proportion of bioavailable plastic-released DOC^{17,44,45}, we also modify this equation with the bioavailable fraction Bio_i . We

use the average value of percentage of bioavailability from laboratory studies as shown in Supplementary Table 9. Plastic-released DOC may disturb the marine carbon cycle in both ways and further affect the air-to-sea CO₂ exchange. Therefore, we use the change of oceanic CO₂ uptake as an indicator to evaluate the overall impacts.

Growth change of phytoplankton

The detrimental effects of most oceanic plastics on the cell morphology and photosynthesis of phytoplankton may ultimately impact their growth and several laboratory studies have investigated the response of phytoplankton growth rates to plastic concentrations^{17–26,42,46,50–56}. The impacts suggested by laboratory studies are substantial as the concentration of added plastic debris in these studies are relatively high. To investigate the toxicity effect of oceanic plastics, we derive the growth impact parameters from the growth curve or growth data (the former is based on the latter) of phytoplankton under different concentration of plastics from several studies^{17–25,42,46,50–53}. Details about growth impact parameters can be found in Supplementary Tables 6, 7 and 8. We calculate the growth rate of phytoplankton as a function of plastic concentrations:

$$\text{GrowthP}_{ijs} = \text{GrowthI}_{js} \exp(-\text{Param}_{is}P_{ij}) \quad (3)$$

where GrowthP_{ijs} denotes the growth of species s of phytoplankton in grid j under the exposure of polymer type i of plastics. GrowthI_{js} is the original growth rate of species s of phytoplankton in grid j without plastics^{7,33}. Param_{is} is the toxicity effect parameter of polymer type i of oceanic plastics on species s of phytoplankton derived from laboratory studies which are not complete for all plastics and all phytoplankton, so we use the same Param_{is} of PS to represent Param_{is} of ABS for all phytoplankton; use Param_{is} of PE to represent Param_{is} of PP for the growth impacts on *Synechococcus* and *Prochlorococcus*; and use Param_{is} of PVC to represent Param_{is} of PS for the growth impacts on *Prochlorococcus*. The value of Param_{is} not only depends on the polymer type of plastics and the species of phytoplankton but also varies even for the same plastics and the same phytoplankton as a result of different experimental subjects and methods chosen in those laboratory studies^{17–25,42,46,50–53}. We follow this equation to consider the effect of each individual plastic polymer type (the independent toxicity effect scenario). We also investigate the combined toxicity effects of all oceanic plastics on each phytoplankton by multiplying their growth impacts as different polymer types of plastics are dispersed around phytoplankton:

$$\text{GrowthP}_{js} = \text{GrowthI}_{js} \prod \exp(-\text{Param}_{is}P_{ij}) \quad (4)$$

where GrowthP_{js} denotes the growth of species s of phytoplankton in grid j under the exposure of all oceanic plastics. Owing to differences in experimental conditions, different studies may have different results on the toxicity effects of the same polymer type of oceanic plastics on the same phytoplankton species. We select the maximum, middle and minimum parameters to investigate how dose–effect affects the growth impacts of oceanic plastics:

$$\text{GrowthPtoxic}_{js} = \text{GrowthI}_{js} \prod \exp(-\text{Paramtoxic}_{is}P_{ij}) \quad (5)$$

where GrowthPtoxic_{js} is the growth of species s of phytoplankton in grid j under the exposure of all oceanic plastics with maximum, middle or minimum toxicity effect parameters. Paramtoxic_{is} denotes the maximum, middle or minimum toxicity effect parameters of polymer type i of oceanic plastics on species s of phytoplankton for each phytoplankton. We also include the relative size effect by multiplying the relative size effect parameters:

$$\text{GrowthPsize}_{js} = \text{GrowthI}_{js} \prod \exp(-\text{Param}_{is}P_{ij}\text{Paramsize}_{isg}) \quad (6)$$

where GrowthPsize_{js} is the growth of species s of phytoplankton in grid j under the exposure of all oceanic plastics which is modified by the relative size effect. Paramsize_{isg} denotes the relative size effect parameter for each phytoplankton and g denotes the relative size groups. We divide the Paramsize_{isg} into different groups on the basis of both the diameter of different oceanic plastics and the size of phytoplankton. Specifically, there are three groups for diatoms: <0.3125, 0.3125–5, >5 mm; three groups for other large plankton: <0.0781, 0.0781–1.25, >1.25 mm; two groups for *Prochlorococcus* and *Synechococcus*: <0.0781, >0.0781 mm (Supplementary Table 2). Plastic abundance can also affect the growth impacts of oceanic plastics on phytoplankton via higher or lower concentration of oceanic plastics. We include the plastic abundance effect based on different plastic simulation scenarios:

$$\text{GrowthPplastic}_{js} = \text{GrowthI}_{js} \prod \exp(-\text{Param}_{is}P_{ijp}) \quad (7)$$

where $\text{GrowthPplastic}_{js}$ is the growth of species s of phytoplankton in grid j under the exposure of different concentration of oceanic plastics. Parameter P_{ijp} is the concentration of polymer type i of oceanic plastic in grid j (m⁻²) in plastic simulation scenario p .

Scenario settings

We design various scenarios to comprehend the influence of factors such as plastic toxicity parameter settings, uncertainties related to plastic abundance and the role of relative size effects in the process of plastic impacting the marine carbon cycle (Supplementary Table 1). We use the middle plastic abundance as the baseline of oceanic plastic emission to investigate the mean value of plastic-related buried carbon and the impacts of plastic-released DOC (middle DOC-releasing rate is also used) as shown in Figs. 3 and 4. We also estimate the upper and lower bound of buried carbon by adapting the maximum and minimum plastic abundance as shown in Supplementary Table 2. The upper and lower bound of impacts of plastic-released DOC on marine carbon cycle are estimated by using maximum and minimum plastic abundance as well as high and low DOC-releasing rate as shown in Supplementary Table 3. On the basis of the middle plastic abundance, we combine toxicity effects of each plastic on all phytoplankton species as the combined toxicity effect scenario and we select different toxicity effect parameters (maximum (Fig. 4b(i)–(v)), minimum and middle (Supplementary Fig. 1a(i)–(iv) and b(i)–(iv))) for evaluating uncertainties; we design the independent toxicity effect scenario to investigate how oceanic plastic with single polymer type (PE, PP, PVC, PS and ABS) impacts marine phytoplankton individually (Supplementary Fig. 2a(i)–(v)); we consider the relative size effect of plastic–phytoplankton pairs by setting different relative size pair groups as the relative size effect scenario (Supplementary Fig. 3a(i)–(v) and Supplementary Table 4). Then, we combine the middle toxicity effect parameters with maximum and minimum oceanic plastic emission as plastic abundance (maximum) scenario (Supplementary Fig. 5a(i)–(v)) and plastic abundance (minimum) scenario (Supplementary Fig. 4b(i)–(v)). We also investigate the joint impacts of maximum toxicity effects and maximum plastic abundance by combining toxicity effect parameters from the combined toxicity effect scenario (maximum) and oceanic plastic emission of plastic abundance (maximum) scenario as the combined toxicity effect scenario (maximum) and plastic abundance (maximum) scenario (Supplementary Fig. 5a(i)–(v)). Plastic-released DOC may also contribute to air-to-sea CO₂ flux change in these toxicity-related scenarios as it can be used by microbes as nutrients. However, we consider the interactions with nutrient demand by phytoplankton are rather small as carbon is not a typical limiting nutrient for phytoplankton growth. In addition, plastic-released-DOC is also much smaller than the existing plankton-derived. Thus, we only present results of one scenario which incorporate the impact of plastic-released DOC into the impact of plastics toxicity effects on the oceanic CO₂ uptake change

simultaneously as the combined toxicity effect (include DOC) scenario (Supplementary Table 1).

Model sensitivity

We test the sensitivity of model results of air-to-sea CO₂ flux change to key model parameters as depicted in Supplementary Table 9 and Supplementary Fig. 7. Sensitivity of plastic DOC releasing is tested by using different DOC-releasing rates, plastic abundance, as well as considering bioavailable scenario as shown in Supplementary Fig. 7a. We also tested sensitivity of plastic toxicity effects to plastic abundance, toxicity effect parameter, size effect and DOC-releasing effect (Supplementary Fig. 7b).

Reporting summary

Further information on research design is available in the Nature Portfolio Reporting Summary linked to this article.

Data availability

All data are available in the Article, Supplementary Information or via Zenodo at <https://zenodo.org/records/16722412> (ref. 57). Correspondence should be addressed to Y.Z.

Code availability

All model code is available via Zenodo at <https://zenodo.org/records/16722412> (ref. 57).

References

- Zhang, Y. et al. Plastic waste discharge to the global ocean constrained by seawater observations. *Nat. Commun.* **14**, 1372 (2023).
- Fu, Y. et al. Modeling atmospheric microplastic cycle by GEOS-Chem: an optimized estimation by a global dataset suggests likely 50 times lower ocean emissions. *One Earth* **6**, 705–714 (2023).
- Kooi, M., Nes, E. H. V., Scheffer, M. & Koelmans, A. A. Ups and downs in the ocean: effects of biofouling on vertical transport of microplastics. *Environ. Sci. Technol.* **51**, 7963–7971 (2017).
- Allen, S. et al. Evidence of free tropospheric and long-range transport of microplastic at Pic du Midi Observatory. *Nat. Commun.* **12**, 7242 (2021).
- Cressey, D. Bottles, bags, ropes and toothbrushes: the struggle to track ocean plastics. *Nature* **536**, 263–265 (2016).
- Galgani, L. & Loiseau, S. A. Plastic pollution impacts on marine carbon biogeochemistry. *Environ. Pollut.* **268**, 115598 (2021).
- Dutkiewicz, S., Follows, M. J. & Bragg, J. G. Modeling the coupling of ocean ecology and biogeochemistry. *Glob. Biogeochem. Cycles* **23**, 2008GB003405 (2009).
- Moran, M. A. et al. Deciphering ocean carbon in a changing world. *Proc. Natl Acad. Sci. USA* **113**, 3143–3151 (2016).
- Galgani, L. et al. Hitchhiking into the deep: how microplastic particles are exported through the biological carbon pump in the North Atlantic Ocean. *Environ. Sci. Technol.* **56**, 15638–15649 (2022).
- Roberts, C. et al. Microplastics may reduce the efficiency of the biological carbon pump by decreasing the settling velocity and carbon content of marine snow. *Limnol. Oceanogr.* **69**, 1918–1928 (2024).
- Wu, N., Grieve, S. W. D., Manning, A. J. & Spencer, K. L. Flocs as vectors for microplastics in the aquatic environment. *Nat. Water* **2**, 1082–1090 (2024).
- IPCC. *Climate Change 2021: The Physical Science Basis* (Cambridge Univ. Press, 2023).
- Regnier, P. et al. Anthropogenic perturbation of the carbon fluxes from land to ocean. *Nat. Geosci.* **6**, 597–607 (2013).
- Alongi, D. M. *Blue Carbon* (Springer, 2018).
- Smeaton, C. Augmentation of global marine sedimentary carbon storage in the age of plastic. *Limnol. Oceanogr. Lett.* **6**, 113–118 (2021).
- Romera-Castillo, C., Pinto, M., Langer, T. M., Álvarez-Salgado, X. A. & Herndl, G. J. Dissolved organic carbon leaching from plastics stimulates microbial activity in the ocean. *Nat. Commun.* **9**, 1430 (2018).
- Kvale, K., Hunt, C., James, A. & Koeve, W. Regionally disparate ecological responses to microplastic slowing of faecal pellets yields coherent carbon cycle response. *Front. Mar. Sci.* **10**, 1111838 (2023).
- Galgani, L. et al. Marine plastics alter the organic matter composition of the air–sea boundary layer, with influences on CO₂ exchange: a large-scale analysis method to explore future ocean scenarios. *Sci. Total Environ.* **857**, 159624 (2023).
- Sendra, M., Rodríguez-Romero, A., Yeste, M. P., Blasco, J. & Tovar-Sánchez, A. Products released from surgical face masks can provoke cytotoxicity in the marine diatom *Phaeodactylum tricornutum*. *Sci. Total Environ.* **841**, 156611 (2022).
- Zhu, Z. et al. Joint toxicity of microplastics with triclosan to marine microalgae *Skeletonema costatum*. *Environ. Pollut.* **246**, 509–517 (2019).
- Zhao, T. et al. Microplastic-induced apoptosis and metabolism responses in marine dinoflagellate, *Karenia mikimotoi*. *Sci. Total Environ.* **804**, 150252 (2022).
- Tetu, S. G. et al. Plastic leachates impair growth and oxygen production in *Prochlorococcus*, the ocean's most abundant photosynthetic bacteria. *Commun. Biol.* **2**, 184 (2019).
- Ge, J. et al. Microplastics impacts in seven flagellate microalgae: role of size and cell wall. *Environ. Res.* **206**, 112598 (2022).
- Chae, Y., Kim, D. & An, Y.-J. Effects of micro-sized polyethylene spheres on the marine microalga *Dunaliella salina*: focusing on the algal cell to plastic particle size ratio. *Aquat. Toxicol.* **216**, 105296 (2019).
- Lagarde, F. et al. Microplastic interactions with freshwater microalgae: hetero-aggregation and changes in plastic density appear strongly dependent on polymer type. *Environ. Pollut.* **215**, 331–339 (2016).
- Galgani, L. et al. Microplastics increase the marine production of particulate forms of organic matter. *Environ. Res. Lett.* **14**, 124085 (2019).
- Machado, M. C., Vimbela, G. V., Silva-Oliveira, T. T., Bose, A. & Tripathi, A. The response of *Synechococcus* sp. PCC 7002 to micro-/nano polyethylene particles—investigation of a key anthropogenic stressor. *PLoS ONE* **15**, e0232745 (2020).
- Follows, M. J., Dutkiewicz, S., Grant, S. & Chisholm, S. W. Emergent biogeography of microbial communities in a model ocean. *Science* **315**, 1843–1846 (2007).
- Athanasios, P. et al. Global distribution of nearshore slopes with implications for coastal retreat. *Earth Syst. Sci. Data* **11**, 1515–1529 (2019).
- Geyer, R., Jambeck, J. R. & Law, K. L. Production, use, and fate of all plastics ever made. *Sci. Adv.* **3**, e1700782 (2017).
- Lebreton, L. The status and fate of oceanic garbage patches. *Nat. Rev. Earth Environ.* **3**, 730–732 (2022).
- Mai, L. et al. Global riverine plastic outflows. *Environ. Sci. Technol.* **54**, 10049–10056 (2020).
- Feng, L.-J. et al. Short-term exposure to positively charged polystyrene nanoparticles causes oxidative stress and membrane destruction in cyanobacteria. *Environ. Sci. Nano* **6**, 3072–3079 (2019).
- Lebreton, L. C. M. et al. River plastic emissions to the world's oceans. *Nat. Commun.* **8**, 15611 (2017).
- Zheng, J. & Suh, S. Strategies to reduce the global carbon footprint of plastics. *Nat. Clim. Change* **9**, 374–378 (2019).

36. Jambeck, J. R. et al. Plastic waste inputs from land into the ocean. *Science* **347**, 768–771 (2015).
37. Flombaum, P. et al. Present and future global distributions of the marine cyanobacteria *Prochlorococcus* and *Synechococcus*. *Proc. Natl Acad. Sci. USA* **110**, 9824–9829 (2013).
38. World Bank Group. CO₂ emissions (kt). *World Bank Open Data* <https://data.worldbank.org> (2023).
39. Zhu, L., Zhao, S., Bittar, T. B., Stubbins, A. & Li, D. Photochemical dissolution of buoyant microplastics to dissolved organic carbon: rates and microbial impacts. *J. Hazard. Mater.* **383**, 121065 (2020).
40. Ziervogel, K. et al. Microbial interactions with microplastics: insights into the plastic carbon cycle in the ocean. *Mar. Chem.* **262**, 104395 (2024).
41. DeAngelo, J. et al. Energy systems in scenarios at net-zero CO₂ emissions. *Nat. Commun.* **12**, 6096 (2021).
42. Kvale, K., Prowe, A. E. F., Chien, C.-T., Landolfi, A. & Oschlies, A. Zooplankton grazing of microplastic can accelerate global loss of ocean oxygen. *Nat. Commun.* **12**, 2358 (2021).
43. Intergovernmental negotiating committee on plastic pollution. *UNEP* <https://www.unep.org/inc-plastic-pollution> (2024).
44. Lee, Y. K., Murphy, K. R. & Hur, J. Fluorescence signatures of dissolved organic matter leached from microplastics: polymers and additives. *Environ. Sci. Technol.* **54**, 11905–11914 (2020).
45. Zhao, T., Tan, L., Huang, W. & Wang, J. The interactions between micro polyvinyl chloride (mPVC) and marine dinoflagellate *Karenia mikimotoi*: the inhibition of growth, chlorophyll and photosynthetic efficiency. *Environ. Pollut.* **247**, 883–889 (2019).
46. Tréguer, P. et al. Influence of diatom diversity on the ocean biological carbon pump. *Nat. Geosci.* **11**, 27–37 (2018).
47. Marshall, J., Adcroft, A., Hill, C., Perelman, L. & Heisey, C. A finite-volume, incompressible Navier Stokes model for studies of the ocean on parallel computers. *J. Geophys. Res. Oceans* **102**, 5753–5766 (1997).
48. Kroodsma, D. A. et al. Tracking the global footprint of fisheries. *Science* **359**, 904–908 (2018).
49. Wang, X. et al. Ship emissions around China under gradually promoted control policies from 2016 to 2019. *Atmos. Chem. Phys.* **21**, 13835–13853 (2021).
50. Weiss, L. et al. The missing ocean plastic sink: gone with the rivers. *Science* **373**, 107–111 (2021).
51. Smith, W. O. The relative importance of chlorophyll, dissolved and particulate material, and seawater to the vertical extinction of light. *Estuar. Coast. Shelf Sci.* **15**, 459–465 (1982).
52. Su, Y. et al. Microplastic exposure represses the growth of endosymbiotic dinoflagellate *Cladocopium goreau* in culture through affecting its apoptosis and metabolism. *Chemosphere* **244**, 125485 (2020).
53. Ripken, C., Khalturin, K. & Shoguchi, E. Response of coral reef dinoflagellates to nanoplastics under experimental conditions suggests downregulation of cellular metabolism. *Microorganisms* **8**, 1759 (2020).
54. Liu, G., Jiang, R., You, J., Muir, D. C. G. & Zeng, E. Y. Microplastic impacts on microalgae growth: effects of size and humic acid. *Environ. Sci. Technol.* **54**, 1782–1789 (2020).
55. Zhang, C., Chen, X., Wang, J. & Tan, L. Toxic effects of microplastic on marine microalgae *Skeletonema costatum*: interactions between microplastic and algae. *Environ. Pollut.* **220**, 1282–1288 (2017).
56. Focardi, A. et al. Plastic leachates impair picophytoplankton and dramatically reshape the marine microbiome. *Microbiome* **10**, 179 (2022).
57. PANG, Q. Code and data for ‘The potential impacts of plastic on the marine carbon cycle’. *Zenodo* <https://doi.org/10.5281/zenodo.16722411> (2025).

Acknowledgements

We appreciate A. T. Schartup and E. Zakem for the helpful discussions and suggestions. This study is supported by the Postgraduate Research and Practice Innovation Program of Jiangsu Province (KYCX23_0125) (to Q.P.). L.G. was supported by the Italian Ministry of University and Research funded by the European Union-Next Generation EU, project code CN_00000033, CUP B63 C22000650007, project title ‘National Biodiversity Future Center-NBFC’.

Author contributions

Conceptualization: Y.Z., Q.P. Methodology: Q.P., P.W., X.W., Z.Z., T.Y. Investigation: Q.P., P.W. Visualization: Q.P., P.W., X.W. Funding acquisition: Q.P. Project administration: Y.Z. Supervision: Y.Z. Writing—original draft: Q.P., Y.Z. Writing—review and editing: Y.Z., Q.P., L.G., T.Y., H.W.

Competing interests

The authors declare no competing interests.

Additional information

Supplementary information The online version contains supplementary material available at <https://doi.org/10.1038/s41893-025-01632-7>.

Correspondence and requests for materials should be addressed to Yanxu Zhang.

Peer review information *Nature Sustainability* thanks the anonymous reviewers for their contribution to the peer review of this work.

Reprints and permissions information is available at www.nature.com/reprints.

Publisher's note Springer Nature remains neutral with regard to jurisdictional claims in published maps and institutional affiliations.

Springer Nature or its licensor (e.g. a society or other partner) holds exclusive rights to this article under a publishing agreement with the author(s) or other rightsholder(s); author self-archiving of the accepted manuscript version of this article is solely governed by the terms of such publishing agreement and applicable law.

© The Author(s), under exclusive licence to Springer Nature Limited 2025

Reporting Summary

Nature Portfolio wishes to improve the reproducibility of the work that we publish. This form provides structure for consistency and transparency in reporting. For further information on Nature Portfolio policies, see our [Editorial Policies](#) and the [Editorial Policy Checklist](#).

Statistics

For all statistical analyses, confirm that the following items are present in the figure legend, table legend, main text, or Methods section.

n/a	Confirmed
<input checked="" type="checkbox"/>	<input type="checkbox"/> The exact sample size (<i>n</i>) for each experimental group/condition, given as a discrete number and unit of measurement
<input checked="" type="checkbox"/>	<input type="checkbox"/> A statement on whether measurements were taken from distinct samples or whether the same sample was measured repeatedly
<input checked="" type="checkbox"/>	<input type="checkbox"/> The statistical test(s) used AND whether they are one- or two-sided <i>Only common tests should be described solely by name; describe more complex techniques in the Methods section.</i>
<input checked="" type="checkbox"/>	<input type="checkbox"/> A description of all covariates tested
<input checked="" type="checkbox"/>	<input type="checkbox"/> A description of any assumptions or corrections, such as tests of normality and adjustment for multiple comparisons
<input type="checkbox"/>	<input checked="" type="checkbox"/> A full description of the statistical parameters including central tendency (e.g. means) or other basic estimates (e.g. regression coefficient) AND variation (e.g. standard deviation) or associated estimates of uncertainty (e.g. confidence intervals)
<input checked="" type="checkbox"/>	<input type="checkbox"/> For null hypothesis testing, the test statistic (e.g. <i>F</i> , <i>t</i> , <i>r</i>) with confidence intervals, effect sizes, degrees of freedom and <i>P</i> value noted <i>Give P values as exact values whenever suitable.</i>
<input checked="" type="checkbox"/>	<input type="checkbox"/> For Bayesian analysis, information on the choice of priors and Markov chain Monte Carlo settings
<input checked="" type="checkbox"/>	<input type="checkbox"/> For hierarchical and complex designs, identification of the appropriate level for tests and full reporting of outcomes
<input checked="" type="checkbox"/>	<input type="checkbox"/> Estimates of effect sizes (e.g. Cohen's <i>d</i> , Pearson's <i>r</i>), indicating how they were calculated

Our web collection on [statistics for biologists](#) contains articles on many of the points above.

Software and code

Policy information about [availability of computer code](#)

Data collection	Both custom codes from the NJU-MP model and the Darwin ecosystem model were used to collect data in this study, and no software was used for data collection.
Data analysis	Custom codes of MATLAB were used to analyze data in this study, and MATLAB R2021b (9.11.0.1769968) was used for data analysis.

For manuscripts utilizing custom algorithms or software that are central to the research but not yet described in published literature, software must be made available to editors and reviewers. We strongly encourage code deposition in a community repository (e.g. GitHub). See the Nature Portfolio [guidelines for submitting code & software](#) for further information.

Data

Policy information about [availability of data](#)

All manuscripts must include a [data availability statement](#). This statement should provide the following information, where applicable:

- Accession codes, unique identifiers, or web links for publicly available datasets
- A description of any restrictions on data availability
- For clinical datasets or third party data, please ensure that the statement adheres to our [policy](#)

All data supporting the findings are available in the article, the supplementary materials, or the website: <https://ebmg.tulane.edu/models/plastic/>.

Human research participants

Policy information about [studies involving human research participants and Sex and Gender in Research](#).

Reporting on sex and gender

Use the terms sex (biological attribute) and gender (shaped by social and cultural circumstances) carefully in order to avoid confusing both terms. Indicate if findings apply to only one sex or gender; describe whether sex and gender were considered in study design whether sex and/or gender was determined based on self-reporting or assigned and methods used. Provide in the source data disaggregated sex and gender data where this information has been collected, and consent has been obtained for sharing of individual-level data; provide overall numbers in this Reporting Summary. Please state if this information has not been collected. Report sex- and gender-based analyses where performed, justify reasons for lack of sex- and gender-based analysis.

Population characteristics

Describe the covariate-relevant population characteristics of the human research participants (e.g. age, genotypic information, past and current diagnosis and treatment categories). If you filled out the behavioural & social sciences study design questions and have nothing to add here, write "See above."

Recruitment

Describe how participants were recruited. Outline any potential self-selection bias or other biases that may be present and how these are likely to impact results.

Ethics oversight

Identify the organization(s) that approved the study protocol.

Note that full information on the approval of the study protocol must also be provided in the manuscript.

Field-specific reporting

Please select the one below that is the best fit for your research. If you are not sure, read the appropriate sections before making your selection.

☐ Life sciences ☐ Behavioural & social sciences ☒ Ecological, evolutionary & environmental sciences

For a reference copy of the document with all sections, see [nature.com/documents/nr-reporting-summary-flat.pdf](https://www.nature.com/documents/nr-reporting-summary-flat.pdf)

Ecological, evolutionary & environmental sciences study design

All studies must disclose on these points even when the disclosure is negative.

Study description

We designed scenarios with or without oceanic plastics to investigate oceanic plastics' impacts on marine carbon cycle. For different scenarios, the mass, distribution, size, type of oceanic plastics are different.

Research sample

We used global oceanic plastics data from the modeling results of the NJU-MP model, which originates from <https://doi.org/10.1038/s41467-023-37108-5> for this research.

Sampling strategy

Our research data includes the whole global oceanic plastics.

Data collection

All data involved was collected from the modeling results of the NJU-MP model and the Darwin ecosystem model.

Timing and spatial scale

The start and stop of data collection is same as we collected these data from modeling outputs

Data exclusions

No data is excluded.

Reproducibility

Please use the the NJU-MP model and the Darwin ecosystem model to repeat results of this study.

Randomization

It is not relevant to our study as we modeled the oceanic plastics, marine phytoplankton, and marine carbon cycle of the whole global ocean.

Blinding

It is not relevant to our study as we modeled the oceanic plastics, marine phytoplankton, and marine carbon cycle of the whole global ocean.

Did the study involve field work? ☐ Yes ☒ No

Reporting for specific materials, systems and methods

We require information from authors about some types of materials, experimental systems and methods used in many studies. Here, indicate whether each material, system or method listed is relevant to your study. If you are not sure if a list item applies to your research, read the appropriate section before selecting a response.

Materials & experimental systems

n/a	Involved in the study
<input checked="" type="checkbox"/>	<input type="checkbox"/> Antibodies
<input checked="" type="checkbox"/>	<input type="checkbox"/> Eukaryotic cell lines
<input checked="" type="checkbox"/>	<input type="checkbox"/> Palaeontology and archaeology
<input checked="" type="checkbox"/>	<input type="checkbox"/> Animals and other organisms
<input checked="" type="checkbox"/>	<input type="checkbox"/> Clinical data
<input checked="" type="checkbox"/>	<input type="checkbox"/> Dual use research of concern

Methods

n/a	Involved in the study
<input checked="" type="checkbox"/>	<input type="checkbox"/> ChIP-seq
<input checked="" type="checkbox"/>	<input type="checkbox"/> Flow cytometry
<input checked="" type="checkbox"/>	<input type="checkbox"/> MRI-based neuroimaging